
Learning to Search and Searching to Learn for Generalization in Planning

Michael Aichmüller*¹ Yannik Hesse*¹ Hector Geffner¹

Abstract

Combinatorial generalization remains a central challenge in Deep Reinforcement Learning (DRL). Classical planning provides a simple yet challenging setting to study this problem through explicit relational descriptions, without requiring learning from perception. In sparse-reward domains, standard RL exploration via real-time search is ineffective, and learning-based planning methods often rely on expert demonstrations, hindsight relabeling, or random walks from the goal state. In contrast, planners rely on best-first search methods such as A* to solve problems from scratch. We propose a self-improving WA* learning framework in combination with a value heuristic represented by a Relational Graph Neural Network: the heuristic guides search, and the resulting search data updates the heuristic via Q -learning. This loop yields heuristics that can function as general policies and solve new instances even without search, where DRL otherwise fails, as we show on puzzles such as Sokoban, Push-World, The Witness, and the 2023 International Planning Competition benchmarks. Notably, we demonstrate strong zero-shot generalization: For example, heuristics trained on Blocksworld instances with fewer than 30 blocks successfully solve instances with 488 blocks without search.

1. Introduction

Combinatorial generalization is a key challenge in deep reinforcement learning where the learned policies or value functions are expected to generalize out-of-distribution due to a common problem structure (Kirk et al., 2023; Lake & Baroni, 2023; Mohan et al., 2024). Classical planning is an ideal setting for studying and addressing this problem

*Equal contribution ¹Department of Machine Learning and Reasoning, RWTH Aachen University, Aachen, Germany. Correspondence to: Michael Aichmüller <michael.aichmueller@ml.rwth-aachen.de>.

because the common problem structure is given and does not need to be learned from pixels (Russell & Norvig, 2020; Ghallab et al., 2016; Geffner & Bonet, 2013). A planning *domain* specifies a fixed relational vocabulary and action schemas, while *instances* vary in the number of objects, the initial state, and the goal. This clean domain–instance separation induces systematic out-of-distribution shifts, including changes in branching factor and required search depth, and makes classical planning a natural testbed for *generalization across states, goals, and problem size* (formal definitions in Section 3).

Many challenging learning tasks in the setting of classical planning involve generalization, including learning a domain from traces drawn from hidden domain instances (Arora et al., 2018; Xi et al., 2024; Gösgens et al., 2025), and closer to the aims of this work, learning general policies and heuristics (Toyer et al., 2020; Rivlin et al., 2020; Garg et al., 2020; Karia & Srivastava, 2022; Chen et al., 2024). A general policy is a policy that can be used to solve arbitrary instances of the domain without search, and a general heuristic is an estimator of the cost to the goal which can be effectively used to search for plans in any domain instance. In recent years, DRL approaches have been used to learn general policies and heuristics over given domains (Rivlin et al., 2020; Ståhlberg et al., 2023a; Ståhlberg & Geffner, 2026). Yet, real-time search as used in these algorithms, moving iteratively from one state to a successor state (Korf, 1990; Koenig, 2001), is not an effective way to search for plans. Planners use best-first algorithms like WA* or Greedy BFS (Richter & Westphal, 2010; Geffner & Bonet, 2013; Ghallab et al., 2016), and recent approaches have shown indeed the performance gains that can be obtained by combining Bellman updates with best-first search, which is feasible when the model is known (Agostinelli et al., 2019; Orseau & Lelis, 2021).

Early algorithms that combine full Bellman updates with real-time search include Learning Real-Time A* (LRTA*), for deterministic MDPs, and Real-Time Dynamic Programming (RTDP), for stochastic MDPs (Korf, 1990; Barto et al., 1995). RL algorithms, which can be regarded as model-free variants, retain the real-time search, which is crucial when interacting with a world or simulator, but unnecessary when the model is known (Sutton & Barto, 2018). In this case, learning can be improved by considering forms of best-first

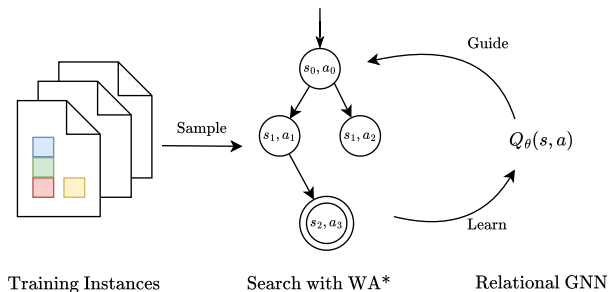


Figure 1. Generalized search for planning. During training, classical planning instances are solved with a search guided by learned $Q(s, a)$ values, which are then updated to improve performance on other instances. Unlike standard RL, (i) exploration uses best-first search (WA*) rather than stepwise real-time search, and (ii) instances vary in both initial state/goal and number of objects.

search, in particular, when the reward (the goal) is sparse. In this work, we push this idea further by learning to search for plans over the whole class of instances defined by a given planning domain. The goal is a self-improving, generalizing learning cycle: starting from a non-informative heuristic, a search for the goal on one instance yields a better heuristic, which then guides search on progressively larger instances.

In the paper, we formulate this form of self-improving generalized search (see Figure 1) that can be applied to families of path-finding problems, uniformly modeled as instances of a common planning domain. For this, general Q -value functions represented with relational GNNs are learned by solving training instances with search, using the states deemed relevant for updating the Q -functions. The self-reinforcing cycle between search and learning appears in a number of research threads in search and RL, but these forms of learning have been tied to one specific state space without generalizing systematically to others. The exceptions are recent works in classical planning for learning general policies and heuristics, yet the former rely on standard RL algorithms and hence real-time search (Rivlin et al., 2020; Ståhlberg et al., 2023a) while the latter rely on supervised learning, and do not benefit from the self-improving learning cycle of better heuristics to guide more efficient searches (Chen, 2025; Horčík et al., 2025).

There are three distinct forms of *generalization* in RL and planning: generalization to other *states*, which is required for RL to scale to large state spaces (Silver et al., 2016; 2017); generalization to other *states and goals*, as in goal-conditioned RL (Schaul et al., 2015; Andrychowicz et al., 2017); and generalization to *states, goals, and problem size*, as pursued in this work.

The paper is organized as follows: we present next the related work, background, and the generalized search for plan-

ning framework, followed by our experiments on different benchmarks and the conclusions we draw¹.

2. Related Work

Planning within RL. The Alpha family of RL algorithms (Silver et al., 2016; 2017; 2018; Schrittwieser et al., 2020) demonstrated the benefits of integrating search into the RL loop. Specifically, Monte Carlo Tree Search (MCTS), guided by value functions and policies learned via actor-critic methods, selects target states for learning, leading to more effective lookaheads and improved learning targets. While this approach performs well in challenging games, MCTS has limitations in our setting: it is ill-suited for single-goal pathfinding, and struggles in non-adversarial puzzle domains where progress depends on sparse or delayed rewards (Orseau & Lelis, 2021). AlphaZero-based general policy learning is studied in the experiments section as well, and results underline these drawbacks.

Learning to Search. Learning Real-Time A* (LRTA*) and Real-time Dynamic Programming (RTDP) are aimed at solving deterministic and stochastic goal-reaching MDPs with a known initial state, combining a greedy real-time search with Bellman updates (Korf, 1990; Barto et al., 1995). If the initial heuristics (cost estimators) are admissible, i.e., do not over-estimate true (expected) costs, and there are no dead-end states from which the goal is not reachable, both LRTA* and RTDP converge to an optimal policy relative to the initial state. More recently, and more closely connected to our work, different best-first search algorithms have been used inside a learning algorithm to solve hard problems like the 5×5 sliding puzzle and the Rubik’s cube (Arfaee et al., 2011; Agostinelli et al., 2019; Orseau & Lelis, 2021; Hadar et al., 2026). The results are impressive but their approaches do not address size generalization.

Learning General Policies. General policies refer to policies that can solve any (solvable) instance of a given planning domain without search (Toyer et al., 2020; Rivlin et al., 2020; Ståhlberg et al., 2023a). Purely symbolic approaches have been developed that result in policies that can be understood and proved correct, but these methods do not scale well (Jiménez et al., 2019; Francès et al., 2021). The most recent works in this thread extend the real-time search in the DRL loop with an adaptation of hindsight experience replay (Andrychowicz et al., 2017) to the planning setting called *lifted* and *propositional HER* (Ståhlberg & Geffner, 2026), where the unachieved goals of a trace are replaced by a suitable relational description of substitute goals actually achieved. However, this form of HER is most effective

¹Code and data are available in the project repository: github.com/maichmueller/generalized-search-for-planning.

when goals can be split into subgoals that can be relabeled; this assumption does not hold uniformly across planning domains and puzzles. In this paper, we build on this work, but replace the real-time search and HER with a best-first search, which is more effective in hard problems.

Learning General Heuristics. Since there are no perfect general policies for intractable domains like Sokoban, a different research thread focuses on learning general heuristic estimators to guide the search for plans in instances of a given domain. In these works, the heuristics $h(s)$ are learned in a supervised way from optimal values $h^*(s)$ precomputed by optimal planners (Ståhlberg et al., 2022; Horčík et al., 2025; Bai et al., 2025). Most approaches use the learned heuristic only to guide search, whereas Bai et al. (2025) additionally exploits the learned GNN representation for symmetry reduction in best-first search by pruning states through hashed GNN embeddings and actions through approximate graph automorphisms. To make learned heuristics more cost-effective, some approaches avoid GNNs altogether and instead use efficient support vector machines over relational Weisfeiler–Leman features, which are closely related to the features computable by GNNs (Chen et al., 2024). Because these methods rely on supervised learning, however, they do not benefit from the self-improving learning cycle of RL approaches.

Search and Exploration in RL. The real-time search used in RL algorithms is often extended with bonuses that reward novel states in the search (Burda et al., 2019; Zhang et al., 2021; Raileanu & Rocktäschel, 2020; Henaff et al., 2022). Indeed, in classical planning, a precise form of novelty, related to a formal notion of problem width, is part of the state-of-the-art planning algorithms as well (Geffner & Lipovetzky, 2012; Lipovetzky & Geffner, 2017; Corrêa & Seipp, 2024). Yet all state-of-the-art search algorithms in classical planning are based on best-first search, not on real-time search where current state is replaced in each step by a successor state (Korf, 1990; Koenig, 2001).

3. Background

Classical Planning. Classical planning problems are deterministic goal-reaching MDPs with extremely sparse rewards and large state spaces. They are expressed in a *language* (PDDL) that separates the description of the *domain* \mathcal{D} from the concrete problem *instances* \mathcal{I} of the domain. The domain specifies relation types (*predicates*) \mathcal{P} , where each predicate $p \in \mathcal{P}$ has arity $\text{ar}(p)$, as well as *action schemas* \mathcal{A} with lifted preconditions and effects defined over these relations (Geffner & Bonet, 2013; Ghallab et al., 2016; Haslum et al., 2019). Instantiating a predicate with objects yields *ground atoms* $p(o_1, \dots, o_{\text{ar}(p)})$, and instantiating an action schema with objects yields a *ground action*

$a(\bar{o})$. An instance \mathcal{I} provides the object set \mathcal{O} , the initial state s_0 , and a goal specification g . The states s are represented by sets of ground atoms; namely, those which are true in the state. Preconditions and goals are conjunctions of literals, and a goal state is a state that includes all the goal atoms. A plan is a sequence of applicable actions that maps s_0 to a goal state.

For example, in *Blocksworld*, a 3-block environment is an instance with objects $\mathcal{O} = \{b_1, b_2, b_3\}$ where the states are described by means of 4 domain predicates: $\text{on}(\cdot, \cdot)$, $\text{ontable}(\cdot)$, $\text{clear}(\cdot)$, and $\text{holding}(\cdot)$. The initial state with a single tower with b_3 at the top, b_2 in the middle, and b_1 on the table would be $s_0 = \{\text{on}(b_3, b_2), \text{on}(b_2, b_1), \text{clear}(b_3), \text{ontable}(b_1)\}$, and the goal can be given by a single ground atom like $\text{on}(b_1, b_2)$ or by a conjunction of many such atoms. Two of the four action schemas in the domain are $\text{stack}(x, y)$, and $\text{unstack}(x, y)$, that ground in actions like $\text{stack}(b_1, b_3)$ and $\text{unstack}(b_3, b_2)$. Only the latter action is applicable in s_0 .

Generalized Planning and Search. In generalized planning, we seek a general policy that can solve any domain instance. These instances vary in the initial state, goals, and number of objects, but the ground actions are instances of the same action schemas, and the states are all described in terms of the same set of predicates. This is what enables generalization while defining very precisely the scope of the generalization sought. In domains where learning with a nearly perfect compact policy is hard or impossible, such as Sokoban (Dor & Zwick, 1999), search aims at learning heuristics that speed up the search in any instance of the given domain. The approach developed in this paper serves these two purposes: it can yield nearly-perfect general policies that require no search or informed heuristic estimators.

Search vs. Real-Time search. In RL and in a number of algorithms like LRTA* and RTDP, one searches for the goal using real-time search, also called agent-based search (Korf, 1990; Koenig, 2001). In this type of search, there is a current state s in each iteration such that, in the next iteration, the current state s' is reachable from s by performing one of the applicable actions in s . If the *dynamic model of the problem is known*, however, a common preferred alternative is to search *best-first* as in A*, WA*, and GBFS (Russell & Norvig, 2020). Best-first search algorithms explore the space more systematically, are not affected by dead-ends, and are complete. In each iteration, they all pick the node n from the search boundary that has the minimum evaluation function $f(n)$. In A*, $f(n) = g(n) + h(n)$ where $g(n)$ is the accumulated cost to reach the node n from the root node, in WA*, it is $f(n) = g(n) + wh(n)$ with $w > 1$, giving thus more importance to the estimate of the cost-to-go than to the cost accumulated, while in greedy best-first search

(GBFS)—not to be confused with greedy search (real-time)—the evaluation function is $f(n) = h(n)$.

4. Generalized Search for Planning

In this work, we address exploration in reinforcement learning by relying on *best-first* search, as in classical planning, rather than *real-time* search, as is typical in RL. GSP (Generalized Search for Planning) is an iterative search-and-learn scheme in which training instances are solved with weighted A^* (WA^*) guided by learned Q -values, and the resulting search data is used to improve those Q -values. To support generalization across states, goals, and problem sizes, we represent Q_θ with a relational graph neural network (see Section 5).

GSP maintains a parametric action-value heuristic $Q_\theta(s, a)$ and repeatedly runs WA^* on sampled instances to generate experience. Each search episode expands promising state-action pairs, stores encountered transitions in a replay buffer, and (when available) attaches search-derived lower bounds on return. Q-learning updates Q_θ from this buffer, and the improved Q_θ in turn guides subsequent search episodes more effectively (cf. Figure 1).

Search Episode. For a sampled instance \mathcal{E} with initial state $s_0(\mathcal{E})$, we run a WA^* search over *state-action* nodes (s, a) . The algorithm maintains (i) a search tree rooted at s_0 , (ii) a priority queue \mathcal{F} (the frontier) containing candidate pairs, and (iii) a replay buffer \mathcal{D} that stores tuples (s, a, \underline{R}) whenever a search-derived lower bound \underline{R} on return is available.

We consider unit step rewards $r = -1$ without discounting, so maximizing return corresponds to finding shorter plans. Let $g(s)$ denote the accumulated return of s along the current tree path from s_0 to s , its negative depth in the tree in our setting. We score each frontier pair by

$$f(s, a) = g(s) + w Q_\theta(s, a),$$

where $w \in \mathbb{R}$ is a weighting constant. At each expansion, we pop the pair $(s, a) \in \mathcal{F}$ with the highest score and generate the successor state $s' = a(s)$. We distinguish three types of transitions: dead-end, goal, and non-terminal. If the successor s' is a non-terminal state, we insert each *previously unseen* successor pair (s', a') into the tree and push it onto the frontier with score $f(s', a')$. If s' is a dead-end state (no applicable actions), we assign the parent pair (s, a) a fixed penalty return R_\perp and store (s, a, R_\perp) in \mathcal{D} .

If s' is a goal state, we backtrack from the goal transition (s_T, a_T) to the root along the discovered solution path and assign each encountered pair (s_t, a_t) the actual return-to-go. This provides a lower bound $\underline{R}(s_t, a_t)$ on the optimal return from that pair, since a higher-return (shorter) solution may

exist. We store these pairs together with their lower bounds in \mathcal{D} . The search terminates when it reaches a goal state or exhausts its expansion budget. Pseudocode is given in Algorithm 1 in the appendix.

Q-learning with Search-Derived Lower Bounds. From the replay buffer, we periodically sample batches $(s, a, \underline{R}) \sim \mathcal{D}$ and regress Q_θ toward one-step Bellman targets. Let the bootstrap target be

$$\hat{y}(s, a) = -1 + \max_{a' \in \mathcal{A}(s')} Q_\theta(s', a'),$$

where s' is the successor reached from (s, a) . We then set the learning target y by pair type. For non-terminal pairs, we use $y = \hat{y}(s, a)$ (standard Q-learning), but the search provides two additional supervision signals: dead-end pairs are regressed towards the fixed penalty $y = R_\perp$, while goal-path pairs can bound the targets as

$$y = \max\{\underline{R}, \hat{y}(s, a)\}.$$

Since \underline{R} comes from a concrete solution found by search, it lower-bounds the optimal return for (s, a) ; taking the maximum prevents bootstrap targets from dropping below what search has already achieved and empirically stabilizes learning. Finally, the mean-squared error $\|Q_\theta(s, a) - y\|^2$ is minimized via stochastic gradient descent.

Instance Selection Strategy. Selecting which training instance to solve next is dynamic and consequential: uniform sampling wastes compute on instances that are already solved reliably or are currently out of reach. We therefore maintain three instance pools and sample from them with exponentially increasing weights: *unsolved*, *solved*, and *satisfied*. If a search successfully finds a plan, the instance is placed in *satisfied*. If additionally the expanded-nodes count equals the found plan length, we consider the instance *solved*. Intuitively, instances with suboptimal solutions provide the most informative updates, whereas instances with no solution yet or with near-best solutions contribute less beyond reinforcing existing behavior. Interestingly, if a problem is placed in *solved*, it does not mean it necessarily found the shortest path within the problem, but rather that the heuristic is so confident in guiding the search that no other nodes need to be expanded.

The GSP learning loop dynamics are visualized in Figure 2, which illustrates the number of training instances the WA^* search solved when guided by learned Q-values, along with the number of nodes expanded in these searches. In the three domains (BLOCKSWORLD, SATELLITE, TRANSPORT), it is clear that as learning progresses, more training problems are solved increasingly efficiently within the given search budget. In the fourth domain shown, FLOORTILE, the

learning loop in GSP is not successful in solving all training instances and remains, on average, at high expansion numbers.

5. Representing Q_θ with Relational GNNs

Following earlier works on general policy learning in classical planning (Ståhlberg et al., 2022; 2023b; 2025; Aichmüller & Geffner, 2025; Chen & Thiébaux, 2024; Horčík et al., 2025), and in particular (Ståhlberg & Geffner, 2026), the Q-function is represented as a relational GNN. Planning states are indeed relational structures: a state s is a set of true ground atoms² $p(\bar{o})$ over a finite object set \mathcal{O} , and the goal is a conjunction g of literals. We write $\bar{o} = (o_1, \dots, o_{\text{ar}(p)})$ for an ordered tuple of objects matching the arity of predicate p . In goal-conditioned RL, both the current state and the goal are required to be encoded. To this end, we form a relation set

$$\mathcal{R}_{s,g} := \{p(\bar{o}) \mid p(\bar{o}) \in s \cup g\}.$$

Since our heuristic is action-value based, we make action choices explicit during message passing by augmenting the relational input with auxiliary action-atoms. Concretely, for each applicable grounded action $a = A(\bar{o}) \in \mathcal{A}(s)$ we introduce a dedicated action object o_a (one per applicable action in s) and an atom $A(o_a, \bar{o})$, and define

$$\mathcal{R}_A := \{A(o_a, \bar{o}) \mid a = A(\bar{o}) \in \mathcal{A}(s)\}.$$

The final input is the set $\mathcal{R} = \mathcal{R}_{s,g} \cup \mathcal{R}_A$ of relational facts over the extended object universe $\tilde{\mathcal{O}} = \mathcal{O} \cup \{o_a : a \in \mathcal{A}(s)\}$.

We parameterize $Q_\theta(s, a)$ with a relational message-passing network that maintains a feature embedding $X_i(o) \in \mathbb{R}^d$ for each object o at layer i , initialized to $X_0(o) = \mathbf{0}$. Given \mathcal{R} , embeddings are updated for L layers by exchanging messages along atoms. For each atom $q = p(o_1, \dots, o_{\text{ar}(p)}) \in \mathcal{R}$, a predicate-specific function produces *position-wise* messages

$$(m_{o_1}^q, \dots, m_{o_{\text{ar}(p)}}^q) = \text{Comb}_p(X_i(o_1), \dots, X_i(o_{\text{ar}(p)})),$$

so that the message sent to an object depends on its argument role in the relation. An object o then aggregates all incoming messages across atoms that contain it,

$$m_o = \text{Agg}(\{m_o^q : q \in \mathcal{R}, o \in q\}),$$

where Agg is permutation-invariant. Finally, the embedding is updated with a shared update function and a residual connection,

$$X_{i+1}(o) = X_i(o) + \text{Comb}_U(X_i(o), m_o),$$

²We follow the closed-world assumption, i.e., atoms that are not mentioned in a state s are false.

for $i = 0, \dots, L - 1$.

After L layers, we obtain final embeddings $\{X_L(o)\}$ that are equivariant to object permutations. We compute action-values with a single shared readout that combines the embedding of the action object with a pooled summary of the state and action objects. Let

$$\bar{X}(s, g) = \text{Pool}(\{X_L(o) \mid o \in \tilde{\mathcal{O}}\})$$

be a permutation-invariant pooling of all embeddings. For an action $a \in \mathcal{A}(s)$ with associated action object o_a , we define

$$Q_\theta(s, a) = \text{MLP}_Q([X_L(o_a) \parallel \bar{X}(s, g)]),$$

where $[\cdot \parallel \cdot]$ denotes concatenation. Importantly, MLP_Q is shared across all action schemas; action types and argument structure are expressed through the relational message passing and the resulting embedding $X_L(o_a)$. This way, the model learns a common scoring principle for grounded actions instead of separate schema-specific predictors.

We use smoothmax aggregation and parameterize the update function Comb_U with a single shared multi-layer perceptron (MLP) mapping \mathbb{R}^{2d} to \mathbb{R}^d . In contrast, we implement a separate predicate-specific MLP for each Comb_p , i.e., one MLP per predicate symbol $p \in \mathcal{P}$, mapping $\mathbb{R}^{d \cdot \text{ar}(p)}$ to $\mathbb{R}^{d \cdot \text{ar}(p)}$ and interpreting the output as $\text{ar}(p)$ many position-wise messages in \mathbb{R}^d .

6. Experiments

Our experiments evaluate GSP along two axes: *generalization* to unseen planning instances (varying in size, initial state, and goal) and *exploration efficiency* during training. During training, GSP generates experience via heuristic-guided weighted A^* ($w = 2$). At test time, the learned Q_θ can be used to define a greedy policy or to guide a best-first search. We therefore report results for both greedy execution (GSP_π) and $\text{WA}^*(w = 2)$ guided by Q_θ (GSP_{WA^*}).

We consider three types of domains: planning domains, puzzles, and the PushWorld domain, all described below. Beyond final coverage and plan-quality metrics, we analyze training dynamics by tracking the number of node expansions and instance solve rate over training time, indicating whether learning yields increasingly focused search. Figure 2 shows four exemplary domains, with the remaining domain plots found in the appendix.

Training Setup. The same hyperparameters were used in all experiments. In particular, we use an embedding dimension $d = 32$ and smooth-maximum aggregation. The learning rate is set to 10^{-4} for the R-GNN parameters and 10^{-3} for the readout network. Training is parallelized with

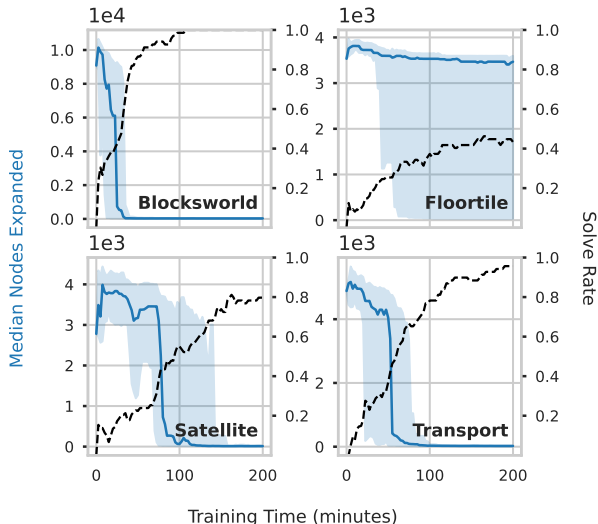


Figure 2. Training progress across selected IPC-learning domains. The blue line (left axis) shows the median number of expanded nodes, with shaded regions representing the 25th and 75th percentiles across all considered training instances. The black line (right axis) shows the solve rate, indicating the percentage of training instances where a goal has been found during training. Each training run lasted 12 hours (720 minutes) of which we show the first 180 minutes here.

one learner process and five search workers that generate experience concurrently. Each search episode uses a 60 s expansion budget and worker-side batching with batch size 256. We use a FIFO replay buffer with a capacity of 40 batches. We use a target network for Q-learning and update it every 10 passes through the replay buffer (Mnih et al., 2015). A detailed overview of how we do final model selection is in the appendix.

6.1. Planning Domains

We use the planning benchmarks from the 2023 International Planning Competition (IPC) learning track. The benchmark comprises 10 domains, each providing 100 training instances (70 used for training and 30 for validation) and 90 test instances. The learning-track instances were designed to stress domain-independent planners by inducing large increases in object counts and applicable actions. For example, in CHILDSNACK, the hardest test instance admits 46,703,541 applicable actions in the initial state, making unguided search infeasible and placing strong pressure on heuristic quality. An overview of scaling is provided in Table 1.

Baselines. We compare against LIFTED HER (Ståhlberg & Geffner, 2026), a method similar to ours that exploits the relational structure using R-GNNs, while learning with real-time search, hindsight relabeling, and DQN (Mnih

Domain	Objects (train/test)	Plan (train/test)
Blocks	29 / 488	102 / 1786
Transport	34 / 453	57 / 1083
Sokoban	11×11 / 99×99 ($b = 3/79$)	22 / 10546
Spanner	28 / 833	80 / 831
Childsnack	51 / 1326	33 / 879
Satellite	27 / 596	41 / 3428
Floortile	9×3 / 34×28 ($r = 2/26$)	105 / 3398
Miconic	21 / 681	24 / 1361
Ferry	25 / 1461	51 / 3895
Rovers	28 / 596	41 / 3428

Table 1. Scaling of problem size across domains. **Objects (train/test)** reports the largest number of objects in any instance of the training and test splits (or domain-specific size parameters for grid domains where applicable: Sokoban uses grid size and boxes b , Floortile grid size and robots r). **Plan (train/test)** reports the number of steps in the (suboptimal) example solutions provided by the 2023 IPC learning benchmark. *These are not used as bounds for training.*

et al., 2015) updates. We further compare with the domain-independent planner LAMA (Richter & Westphal, 2010), and report published solve rates for WL features (WL-f) (Chen, 2025), the state encoding of Horčík et al. (Horčík et al., 2025), and Distincter (Bai et al., 2025). We additionally evaluate an AlphaZero (α_0) policy-value baseline using the same relational network architecture as GSP. Instead of generating data with WA^* , it runs Monte Carlo Tree Search from the current state, using a network policy $\pi_\theta(\cdot | s)$ as a prior over applicable grounded actions and the value head to bootstrap newly expanded leaves. Root visit counts provide the policy target, and the value head is trained on the undiscounted return of the executed episode suffix. We execute the learned policy as a greedy search at test time. This baseline contrasts best-first search with the local MCTS as learning driver for generalized planning.

GSP is evaluated in two test-time modes: greedy execution induced by Q_θ (GSP_π) and WA^* ($w = 2$) guided by Q_θ (GSP_{WA^*}). A secondary experiment establishes a head-to-head comparison with LIFTED HER on the benchmarks used in their evaluation. Details on this can be found in the appendix.

Results. Table 2 summarizes results on IPC 2023 learning-track domains. Greedy execution performs strongly on several domains: GSP_π reaches 100% coverage on BLOCKSWORLD, MICONIC, and SPANNER, surpassing all baselines, and achieves competitive coverage on FERRY (87%) and TRANSPORT (73%), where only LIFTED HER can outperform in both. Against WL-f and Horčík et al., GSP_π is particularly strong on BLOCKSWORLD and MICONIC, while the alternative baselines are stronger on

Domain	GSP $_{\pi}$		GSP $_{WA^*}$		Lifted HER		LAMA		WL-f	Horčík	Distincter	α_0
	Cov.	Steps	Cov.	Steps	Cov.	Steps	Cov.	Steps	Cov.	Cov.	Cov.	Cov.
blocksworld	100%	444	79%	240	98%	421	61%	303	73%	59%	98%	31%
childsack	41%	31	29%	22	40%	35	40%	46	52%	-	71%	0%
ferry	87%	422	77%	232	100%	736	78%	285	73%	66%	92%	19%
floortile	20%	54	28%	57	0%	-	13%	47	3%	32%	2%	0%
miconic	100%	490	98%	268	90%	562	100%	301	98%	68%	100%	28%
rovers	24%	380	11%	17	32%	267	79%	277	50%	33%	47%	0%
satellite	61%	134	33%	18	56%	394	100%	163	57%	40%	53%	0%
sokoban	14%	18	32%	30	8%	11	44%	143	37%	30%	36%	0%
spanner	100%	216	27%	14	97%	160	33%	14	71%	59%	100%	73%
transport	73%	448	57%	52	96%	228	77%	86	56%	39%	56%	0%

Table 2. Results on 2023 IPC benchmark. We report coverage (‘Cov.’ fraction of 90 test instances solved) and average plan length (Steps) over solved instances for GSP as a greedy policy (GSP $_{\pi}$) and as a WA* ($w = 2$) heuristic (GSP $_{WA^*}$), alongside LIFTED HER and LAMA. Published coverage for WL features (WL-f) (Chen, 2025) and Horčík et al. (Horčík et al., 2025) is shown for reference. The GSP budget for each instance is limited to 10,000 expansions or one hour, whichever occurs first.

FLOORTILE and sometimes on CHILDSACK.

Using Q_{θ} as a WA* heuristic yields mixed outcomes. In some domains, WA* improves coverage over greedy execution, most notably in the puzzle domains SOKOBAN (14% \rightarrow 32%) and FLOORTILE (20% \rightarrow 28%). In contrast, WA* reduces coverage on several domains where greedy execution is already strong (e.g., BLOCKSWORLD, SPANNER, and TRANSPORT), indicating that the benchmark’s large branching factors can cause failures, even with effective heuristics.

The two domains, ROVERS and SATELLITE, are solved reliably only by LAMA with 79% and 100% coverage, respectively. This is an expected result due to known limitations of 1-WL expressivity on these domains, which affects all learning-based methods, but not a domain-independent planner like LAMA (Drexler et al., 2024; Horčík & Šír, 2024). CHILDSACK is challenging for all methods, which we attribute primarily to the extreme branching factors discussed above. Distincter is the only method that performs well in this domain, suggesting that symmetry pruning partially counteracts the large branching factor.

In contrast, AlphaZero-style learning did not achieve sufficient generalization, with consistently weak results across domains except in Spanner. This lack of generalization was already visible during training, where runs often failed to generalize to all validation instances. These results support our hypothesis that MCTS is poorly suited as the main search mechanism for general policy learning in this setting. However, we do not exclude that a more targeted study on learning general policies with AlphaZero – particularly one that provides larger simulation budgets, more efficient implementations, and further algorithmic improvements from recent work on AlphaZero – may obtain stronger performance.

The difference in performance between GSP $_{\pi}$ and GSP $_{WA^*}$ on the IPC 2023 benchmark is attributable to two reasons. Firstly, huge branching factors in test instances degrade search, as the benchmark’s design challenges search algorithms specifically. Secondly, the learned heuristic is substantially stronger as a local ranking mechanism than as a global value function on out-of-distribution data. On training problems, the learned heuristic eventually scores well enough globally that the number of expanded nodes is close to or equal to the solution length, indicating that the search is perfectly guided. However, this property deteriorates more quickly than the relative ranking of applicable actions at a state when generalizing to larger or structurally different test instances. As a result, greedy search can remain effective because it relies only on choosing the best local action, whereas WA* must order a frontier using poorly calibrated global scores. This behavior is due to encoding the state together with all applicable actions into a joint relational graph, allowing the GNN to score the actions in direct context to one another, which directly benefits action selection. However, this design does *not* encourage well-calibrated scores across states.

6.2. Puzzles

We next consider combinatorial puzzles that primarily test *structural* (same-size) generalization: 24-PUZZLE, SOKOBAN (10 \times 10, 4 boxes), and THE WITNESS (5 \times 5), following Orseau & Lelis (2021). We use the same training and test splits, but evaluate in a relational setting by converting the environments to PDDL. In contrast to IPC domains, instance sizes are fixed (or vary only mildly); generalization requires transferring relational reasoning to unseen configurations. Notably, unlike the IPC SOKOBAN domain, this version allows arbitrary assignment of boxes to goal locations.

DOMAIN \rightarrow	SOKOBAN / THE WITNESS / SLIDING TILE PUZZLE 5x5																			
MODEL	SOLVED			LENGTH			EXPANSIONS			TIME (s)										
GSP $_{\pi}$	681	/	667	/	0	33.7	/	16.3	/	-	34	/	16	/	-	3.8	/	3.0	/	-
GSP $_{\text{GBFS}, b=1}$	998	/	1000	/	0	38.5	/	16.2	/	-	564	/	496	/	-	59.7	/	84.0	/	-
GSP $_{\text{GBFS}, b=32}$	1000	/	1000	/	-	32.6	/	14.7	/	-	1028	/	722	/	-	103	/	72.0	/	-
GSP $_{\text{WA}^*, w=2, b=1}$	1000	/	1000	/	0	36.0	/	16.0	/	-	207	/	548	/	-	22.1	/	94.2	/	-
GSP $_{\text{WA}^*, w=2, b=32}$	1000	/	1000	/	-	32.5	/	14.7	/	-	972	/	765	/	-	61.1	/	78.7	/	-
LIFTED HER $_{\pi}$	309	/	-	/	0	31.2	/	-	/	-	31	/	-	/	-	-	/	-	/	-
GBFS (\dagger)	914	/	290	/	0	37.7	/	13.3	/	-	5040	/	10128	/	-	49.2	/	44.6	/	-
WA * , $w = 2$ (\dagger)	1000	/	835	/	1000	35.6	/	14.2	/	130.3	3298	/	14305	/	1802	22.8	/	55.5	/	1.5
PHS * (\dagger)	1000	/	1000	/	1000	37.6	/	14.4	/	222.8	1522	/	191	/	2764	11.3	/	1.7	/	3.0
LevinTS (\dagger)	1000	/	1000	/	30	40.1	/	14.8	/	159.6	2640	/	220	/	65545	19.5	/	1.6	/	56.7
PHS $_h$ (\dagger)	1000	/	1000	/	4	38.9	/	14.6	/	119.5	1962	/	222	/	58692	14.8	/	1.8	/	55.3
DEEPCUBE A (\square)	1000	/	-	/	-	32.88	/	-	/	-	1050	/	-	/	-	-	/	-	/	-
LAMA	1000	/	-	/	-	51.60	/	-	/	-	3150	/	-	/	-	-	/	-	/	-

Table 3. Performance comparison on puzzle domains Sokoban (10×10 , 4 boxes) / The Witness (5×5) / Sliding Tile (5×5). ‘Solved’ is the number of solved instances out of 1000 per domain. Length, Expansions, and Time report averages over the solved instances in each domain (‘-’ if results unavailable). Sokoban models were trained on the same training problems as Orseau & Lelis (2021) and DeepCubeA (Agostinelli et al., 2019). All domains are converted to PDDL with relational encoding. LAMA results are taken from Agostinelli et al. (2019) where available. The symbol \dagger refers to Orseau & Lelis (2021), while \square refers to Agostinelli et al. (2019). The GSP budget for each instance is limited to 100,000 expansions or five hours, whichever occurs first. We ran search modes with batch size $b = 1$ and $b = 32$, respectively, allowing a fairer comparison against baselines that reported results with $b = 32$.

Baselines. We compare against established puzzle solvers from Orseau & Lelis (2021), including GBFS, WA * ($w = 2$), and Levin’s policy-guided tree-search variants (LevinTS, PHS * , PHS $_h$). We also report results for DEEPCUBE A on SOKOBAN (Agostinelli et al., 2019) and LAMA where available. For GSP, we report the modes GSP $_{\pi}$, GSP $_{\text{WA}^*}$, and GSP $_{\text{GBFS}}$.

Results. Table 3 summarizes results across all three puzzle domains. While two methods from Orseau & Lelis (2021), WA * and PHS * , were able to solve all of the 24-PUZZLE test instances, GSP did not find a single goal path during training, and subsequently fails at test-time. Finding a solution to one of the training instances is challenging in this domain, as the training instances are not easy and initial Q_{θ} values are not informed. The successful baselines increase their search budgets upon failure during training and, paired with more efficient fixed-size MLPs instead of size-adaptive relational GNNs, are able to eventually find learning signals, while GSP on a fixed budget cannot. Likewise, LIFTED HER is not able to learn successfully.

On SOKOBAN, GSP $_{\pi}$ solves 681/1000 instances, more than double the coverage of LIFTED HER $_{\pi}$ (309). When used for search, GSP $_{\text{WA}^*}$ yields perfect performance, solving all instances with 207 expansions on average, compared to 3298 expansions for WA * ($w = 2$) in Orseau & Lelis (2021) and 1050 expansions for DEEPCUBE A. Similarly, GSP $_{\text{GBFS}}$ reduces the required expansions from 5040 (GBFS baseline) to 564, while simultaneously increasing coverage from 914 to 998/1000.

On THE WITNESS, both GSP $_{\text{WA}^*}$ and GSP $_{\text{GBFS}}$ solve all instances, with expansions in the same range as LevinTS and PHS variants. This pattern is consistent with the importance of dead-end avoidance in this domain: GSP is trained not only from goal-reaching trajectories but also from explicit dead-end states. GSP $_{\pi}$ solves 667 instances, which shows that the learned heuristic is able to surpass even the GBFS baseline (290) in this domain, while losing only to their WA * search (835). Results for DEEPCUBE A and LIFTED HER are not available for THE WITNESS in the cited works, and adapting their training procedures to this setting is non-trivial (reverse walks and goal relabeling depend on unavailable representation structure).

6.3. PushWorld

PushWorld is a Sokoban-like benchmark with sequential pushing and additional object types like composite shapes, and non-goal objects (Kansky et al., 2023). The benchmark is organized into Levels 0–5: Level 0 instances are procedurally generated, whereas Levels 1–5 are hand-designed. We use a custom PDDL formulation (released with our code). We train on Level 0 and evaluate transfer to Level 1, for which it is substantially harder to find generalizing behavior due to highly varying and larger multi-box shapes and the resulting long-horizon spatial reasoning.

Baselines. We compare GSP $_{\pi}$, GSP $_{\text{GBFS}}$, and GSP $_{\text{WA}^*}$ against the model-free RL baselines reported by Kansky et al. (2023) (DQN, PPO) and against LAMA (Richter & Westphal, 2010).

Results. Table 4 summarizes results. As a greedy policy, GSP_{π} solves 93/200 Level 0 test instances, substantially outperforming DQN (20/200) and PPO (11/200), while producing short plans on the solved subset. When used for search, GSP_{WA^*} solves all Level 0 instances (200/200) matching the performance of LAMA in coverage, while yielding higher quality plans on average (18 vs. 24 steps). GSP_{GBFS} solves one instance fewer, but also creates worse plans on average (27 steps) than the WA^* variant and LAMA.

Transfer to Level 1 remains challenging, but Q_{θ} still provides effective search guidance without requiring fine-tuning: GSP_{WA^*} solves 48/63 evaluable instances, with plan lengths again shorter than those of LAMA (26 vs 36 steps) on those instances solved by both methods. Yet, it requires roughly $30\times$ fewer expansions to do so. Again, GSP_{GBFS} performs slightly worse, solving 4 instances fewer and with an overall worse plan quality of 47 steps.

DOMAIN	LEVEL 0 _{ALL} / LEVEL 1			
	SOLVED	LENGTH	EXPANDED	TIME (S)
GSP_{π}	93/5	13/24	13/24	2/8
GSP_{GBFS}	199/44	27/47	1.2K/3.6K	183/1314
GSP_{WA^*}	200/48	18/26	1.8K/3.8K	273/576
PPO	11/4	-/-	-/-	-/-
DQN	20/ ≈ 1	-/-	-/-	-/-
LAMA	200/60	24/40	6.9K/118K	2/41

Table 4. PushWorld test results on Level 0_{ALL} (200) and Level 1 (68). Five Level 1 instances are removed due to requiring a predicate previously unseen during training on level 0. GSP is trained on Level 0 and evaluated on both levels. ‘Solved’ reports solved instances; ‘Length’, ‘Expanded’, and ‘Time’ are averages over solved instances (‘-’ if unavailable), all rounded to integers. LAMA is given 90 GB memory- and 30 minute time budgets per instance. PPO and DQN results are from Kansky et al. (2023). The GSP budget for each instance is limited to 100,000 expansions or five hours, whichever occurs first.

6.4. Ablations

We evaluate the contribution of each training component through three ablations of GSP on the IPC planning domains: removing (i) dead-end supervision, (ii) solution lower-bound targets, and (iii) the priority-based instance sampling strategy. For each ablation, we train five seeds and evaluate the best checkpoint from each seed according to validation performance. We then report mean and standard deviation over the corresponding test results. The full results are shown in Table 8 in the appendix.

Overall, each ablated variant performs worse than the complete model on most domains, although the degradation is usually moderate. The trend is more pronounced for GSP_{π} than for GSP_{WA^*} . This suggests that the search-based evaluator can partially compensate for weaker learned guidance,

while the hardest domains also create floor effects that make ablation differences less visible. Among the components, dead-end supervision has the smallest impact, which is consistent with only a few IPC domains exhibiting dead-ends. Removing solution lower-bound targets causes the largest degradations, indicating that the target bounds aid in avoiding accidental regressions. The priority-based sampling strategy has a smaller effect on mean performance. More generally, the ablations show that similar results can be obtained without each component, but the complete model produces the most stable performance across domains and random seeds.

7. Conclusion

We introduced a simple framework for learning general Q -functions to guide the search for plans on arbitrary instances of a given classical planning domain. The Q -functions, represented by relational GNNs, are learned from instances by performing a best-first (WA^*) search, informed by the Q -values themselves. This creates a self-improving loop in which search provides training targets and the learned heuristic improves subsequent searches. The resulting Q -functions generalize to other domain instances with different states, goals, and numbers of objects, and can be used at test time either as greedy policies or as heuristics for search.

The experiments cover a broad set of domains, ranging from the large, highly scaled instances of the 2023 International Planning Competition to bounded-size combinatorial puzzles and the challenging PushWorld benchmark used to evaluate RL and classical planning algorithms. The performance of GSP competes with the state of the art in almost all of these domains, while addressing this range of problems in a uniform manner, using the same architecture and hyperparameters. The results suggest that best-first search is a useful exploration mechanism for generalized reinforcement learning when the transition model is known, particularly in sparse-reward domains where real-time search struggles to discover informative trajectories.

At the same time, a limitation of the approach is that the learned Q -function is often stronger as a local action-ranking mechanism than as a globally calibrated heuristic over the full search frontier. Improving value generalization across states and combining best-first search with the complementary strengths of real-time search and HER are natural directions for future work.

Impact Statement

This paper presents work whose goal is to advance the field of Machine Learning. There are many potential societal consequences of our work, none of which we feel must be specifically highlighted here.

Acknowledgements

The research has been supported by the Alexander von Humboldt Foundation with funds from the Federal Ministry for Education and Research, Germany. This project has received funding from the European Research Council (ERC) under the European Union’s Horizon 2020 research and innovations programme (Grant agreement No. 885107). This project was also funded by the German Federal Ministry of Education and Research (BMBF) and the Ministry of Culture and Science of the German State of North Rhine-Westphalia (MKW) under the Excellence Strategy of the Federal Government and the Länder.

References

- Agostinelli, F., McAleer, S., Shmakov, A., and Baldi, P. Solving the Rubik’s cube with deep reinforcement learning and search. *Nature Machine Intelligence*, 1:356–363, 2019. doi: 10.1038/s42256-019-0070-z.
- Aichmüller, M. and Geffner, H. Sketch decompositions for classical planning via deep reinforcement learning. In *Proceedings of the 34th International Joint Conference on Artificial Intelligence (IJCAI 2025)*, pp. 8438–8446, 2025.
- Andrychowicz, M., Wolski, F., Ray, A., Schneider, J., Fong, R., Welinder, P., McGrew, B., Tobin, J., Abbeel, P., and Zaremba, W. Hindsight experience replay. In *Proceedings of the 31st Conference on Neural Information Processing Systems (NIPS 2017)*, volume 30, pp. 5048–5058, 2017.
- Arfaee, S. J., Zilles, S., and Holte, R. C. Learning heuristic functions for large state spaces. *Artificial Intelligence*, 175(16-17):2075–2098, 2011.
- Arora, A., Fiorino, H., Pellier, D., Métivier, M., and Pesty, S. A review of learning planning action models. *The Knowledge Engineering Review*, 33, 2018.
- Bai, Y., Thiébaux, S., and Trevizan, F. Learning efficiency meets symmetry breaking. *Proceedings of the International Conference on Automated Planning and Scheduling (ICAPS 2025)*, 35(1):154–159, 2025.
- Barto, A. G., Bradtke, S. J., and Singh, S. P. Learning to act using real-time dynamic programming. *Artificial intelligence*, 72(1-2):81–138, 1995.
- Burda, Y., Edwards, H., Storkey, A., and Klimov, O. Exploration by random network distillation. In *International Conference on Learning Representations (ICLR)*, 2019. URL <https://openreview.net/forum?id=H11JJnR5Ym>.
- Chen, D. Z. Weisfeiler-Leman features for planning: A 1,000,000 sample size hyperparameter study. In *ECAI 2025*. IOS Press, October 2025. doi: 10.3233/FAIA251370. URL <https://doi.org/10.3233/FAIA251370>.
- Chen, D. Z. and Thiébaux, S. Graph learning for numeric planning. In Globerson, A., Mackey, L., Belgrave, D., Fan, A., Paquet, U., Tomczak, J., and Zhang, C. (eds.), *Advances in Neural Information Processing Systems*, volume 37, pp. 91156–91183. Curran Associates, Inc., 2024. doi: 10.52202/079017-2893.
- Chen, D. Z., Thiébaux, S., and Trevizan, F. Learning domain-independent heuristics for grounded and lifted planning. In *Proc. AAAI*, pp. 20078–20086, 2024.
- Corrêa, A. B. and Seipp, J. Consolidating LAMA with best-first width search. *arXiv preprint arXiv:2404.17648*, 2024.
- Dor, D. and Zwick, U. Sokoban and other motion planning problems. *Computational Geometry*, 13(4):215–228, 1999.
- Drexler, D., Ståhlberg, S., Bonet, B., and Geffner, H. Symmetries and expressive requirements for learning general policies. In *Proceedings of the 21st International Conference on Principles of Knowledge Representation and Reasoning (KR 2024)*, 2024.
- Francès, G., Bonet, B., and Geffner, H. Learning general planning policies from small examples without supervision. In *Proceedings of the 35th AAAI Conference on Artificial Intelligence (AAAI 2021)*, pp. 11801–11808, 2021.
- Garg, S., Bajpai, A., et al. Symbolic network: generalized neural policies for relational MDPs. In *International Conference on Machine Learning*, pp. 3397–3407. PMLR, 2020.
- Geffner, H. and Bonet, B. *A concise introduction to models and methods for automated planning*. Morgan & Claypool Publishers, 2013.
- Geffner, H. and Lipovetzky, N. Width and serialization of classical planning problems. In *Proc. ECAI*. IOS Press, 2012.
- Ghallab, M., Nau, D., and Traverso, P. *Automated planning and acting*. Cambridge University Press, 2016.
- Gösgens, J., Jansen, N., and Geffner, H. Learning lifted STRIPS models from action traces alone: A simple, general, and scalable solution. In *Proc. ICAPS*, pp. 189–197, 2025.
- Hadar, G., Agostinelli, F., and Shperberg, S. S. Beyond single-step updates: Reinforcement learning of

- heuristics with limited-horizon search. *Proceedings of the AAAI Conference on Artificial Intelligence*, 40(43):36955–36963, Mar. 2026. doi: 10.1609/aaai.v40i43.41023. URL <https://ojs.aaai.org/index.php/AAAI/article/view/41023>.
- Haslum, P., Lipovetzky, N., Magazzeni, D., Muise, C., Brachman, R., Rossi, F., and Stone, P. *An introduction to the planning domain definition language*, volume 13. Springer, 2019.
- Henaff, M., Raileanu, R., Jiang, M., and Rocktäschel, T. Exploration via elliptical episodic bonuses. In *Advances in Neural Information Processing Systems (NeurIPS)*, 2022.
- Horčík, R., Šír, G., Šimek, V., and Pevný, T. State encodings for GNN-based lifted planners. *Proceedings of the AAAI Conference on Artificial Intelligence*, 39(25):26525–26533, Apr. 2025. doi: 10.1609/aaai.v39i25.34853.
- Horčík, R. and Šír, G. Expressiveness of graph neural networks in planning domains. *Proceedings of the International Conference on Automated Planning and Scheduling*, 34(1):281–289, May 2024. doi: 10.1609/icaps.v34i1.31486. URL <https://ojs.aaai.org/index.php/ICAPS/article/view/31486>.
- Jiménez, S., Segovia-Aguas, J., and Jonsson, A. A review of generalized planning. *The Knowledge Engineering Review*, 34:e5, 2019. doi: 10.1017/S0269888918000231.
- Kansky, K., Vaidyanath, S., Swingle, S., Lou, X., Lázaro-Gredilla, M., and George, D. PushWorld: A benchmark for manipulation planning with tools and movable obstacles. *arXiv preprint arXiv:2301.10289*, 2023.
- Karia, R. and Srivastava, S. Relational abstractions for generalized reinforcement learning on symbolic problems. In *Proc. IJCAI*, 2022.
- Kirk, R., Zhang, A., Grefenstette, E., and Rocktäschel, T. A survey of zero-shot generalisation in deep reinforcement learning. *Journal of Artificial Intelligence Research*, 76:201–264, 2023.
- Koenig, S. Agent-centered search. *AI Magazine*, 22(4):109–109, 2001.
- Korf, R. E. Real-time heuristic search. *Artificial intelligence*, 42(2-3):189–211, 1990.
- Lake, B. M. and Baroni, M. Human-like systematic generalization through a meta-learning neural network. *Nature*, 623(7985):115–121, 2023.
- Lipovetzky, N. and Geffner, H. Best-first width search: Exploration and exploitation in classical planning. In *Proceedings of the AAAI Conference on Artificial Intelligence*, 2017.
- Mnih, V., Kavukcuoglu, K., Silver, D., Rusu, A. A., Veness, J., Bellemare, M. G., Graves, A., Riedmiller, M. A., Fidjeland, A. K., Ostrovski, G., Petersen, S., Beattie, C., Sadik, A., Antonoglou, I., King, H., Kumaran, D., Wierstra, D., Legg, S., and Hassabis, D. Human-level control through deep reinforcement learning. *Nature*, 518:529–533, 2015.
- Mohan, A., Zhang, A., and Lindauer, M. Structure in deep reinforcement learning: A survey and open problems. *Journal of Artificial Intelligence Research*, 79:1167–1236, 2024.
- Orseau, L. and Leis, L. H. S. Policy-guided heuristic search with guarantees. *Proceedings of the AAAI Conference on Artificial Intelligence*, 35(14):12382–12390, May 2021. doi: 10.1609/aaai.v35i14.17469. URL <https://ojs.aaai.org/index.php/AAAI/article/view/17469>.
- Raileanu, R. and Rocktäschel, T. RIDE: Rewarding impact-driven exploration for procedurally-generated environments. In *International Conference on Learning Representations (ICLR)*, 2020. URL <https://openreview.net/forum?id=rkg-TJBFPPB>.
- Richter, S. and Westphal, M. The LAMA planner: Guiding cost-based anytime planning with landmarks. *Journal of Artificial Intelligence Research*, 39:127–177, 2010.
- Rivlin, O., Hazan, T., and Karpas, E. Generalized planning with deep reinforcement learning. *arXiv preprint arXiv:2005.02305*, 2020.
- Russell, S. and Norvig, P. *Artificial Intelligence: A Modern Approach*. Pearson, 2020.
- Schaul, T., Horgan, D., Gregor, K., and Silver, D. Universal value function approximators. In *International Conference on Machine Learning (ICML)*, 2015. URL <https://proceedings.mlr.press/v37/schaul15.html>.
- Schrittwieser, J., Antonoglou, I., Hubert, T., Simonyan, K., Sifre, L., Schmitt, S., Guez, A., Lockhart, E., Hassabis, D., Graepel, T., et al. Mastering ATARI, Go, Chess and Shogi by planning with a learned model. *Nature*, 588(7839):604–609, 2020.
- Silver, D., Huang, A., Maddison, C. J., Guez, A., Sifre, L., van den Driessche, G., Schrittwieser, J., Antonoglou, I., Panneershelvam, V., Lanctot, M., Dieleman, S., Grewe, D., Nham, J., Kalchbrenner, N., Sutskever, I., Lillicrap, T., Leach, M., Kavukcuoglu, K., Graepel, T., and Hassabis, D. Mastering the game of Go with deep neural networks and tree search. *Nature*, 529(7587):484–489, 2016.

- Silver, D., Schrittwieser, J., Simonyan, K., Antonoglou, I., Huang, A., Guez, A., Hubert, T., Baker, L., Lai, M., Bolton, A., Chen, Y., Lillicrap, T., Hui, F., Sifre, L., van den Driessche, G., Graepel, T., and Hassabis, D. Mastering the game of Go without human knowledge. *Nature*, 550(7676):354–359, 2017.
- Silver, D., Hubert, T., Schrittwieser, J., Antonoglou, I., Lai, M., Guez, A., Lanctot, M., Sifre, L., Kumaran, D., Graepel, T., Lillicrap, T., Simonyan, K., and Hassabis, D. A general reinforcement learning algorithm that masters Chess, Shogi, and Go through self-play. *Science*, 362(6419):1140–1144, 2018.
- Ståhlberg, S. and Geffner, H. First-order representation languages for goal-conditioned RL. In *Proceedings of the 40th AAAI Conference on Artificial Intelligence (AAAI 2026)*, 2026.
- Ståhlberg, S., Bonet, B., and Geffner, H. Learning general optimal policies with graph neural networks: Expressive power, transparency, and limits. In *Proceedings of the 32nd International Conference on Automated Planning and Scheduling (ICAPS 2022)*, pp. 629–637, 2022.
- Ståhlberg, S., Bonet, B., and Geffner, H. Learning general policies with policy gradient methods. In *Proc. KR*, pp. 647–657, 2023a.
- Ståhlberg, S., Bonet, B., and Geffner, H. Muninn. In *Learning Track of the International Planning Competition 2023: Planner Abstracts*, 2023b.
- Ståhlberg, S., Bonet, B., and Geffner, H. Learning more expressive general policies for classical planning domains. In *Proceedings of the 39th AAAI Conference on Artificial Intelligence (AAAI 2025)*, pp. 26697–26706, 2025.
- Sutton, R. S. and Barto, A. G. *Reinforcement learning: an introduction*. The MIT Press, Cambridge, Massachusetts, second edition, 2018.
- Toyer, S., Thiébaux, S., Trevizan, F., and Xie, L. ASNets: Deep learning for generalised planning. *Journal of Artificial Intelligence Research (JAIR)*, 68:1–68, 2020.
- Xi, K., Gould, S., and Thiébaux, S. Neuro-symbolic learning of lifted action models from visual traces. In *Proceedings of the International Conference on Automated Planning and Scheduling*, volume 34, pp. 653–662, 2024.
- Zhang, T. et al. NovelD: A simple yet effective exploration criterion. In *Advances in Neural Information Processing Systems (NeurIPS)*, 2021.

A. Appendix

This appendix supplements the main paper with additional material that expands on the presented results. First, we provide a pseudocode implementation of the algorithm introduced in Section 4, shown in Algorithm 1. Second, we include further details on the experimental results and training dynamics for the IPC-Learning domains.

A.1. Detailed Validation Strategy

Model selection is performed using a dedicated validation process. Validation is run concurrently during training, with each run saving its best checkpoint. To ensure robustness, each experiment is repeated across five random seeds, and the overall best-performing checkpoint is selected for reporting.

Within the concurrent validation loop, we periodically load the latest model parameters and evaluate greedy execution on the full validation set. Checkpoints are ranked primarily by validation coverage, with ties broken by the lowest total number of steps on solved instances, and any remaining ties resolved using the lowest RMSE on solved instances. For each experimental setting, we report the single run with the best validation score across all five seeds according to these criteria.

A.2. Training Curves and Training Progress

The IPC-Learning domains are particularly challenging, as successful test-time performance requires strong generalization beyond the training distribution. We summarize the required scaling behavior for these domains in Table 1. Notably, our model successfully solves all BLOCKS instances, including the most difficult test case consisting of 488 blocks.

We additionally present training curves for all IPC-Learning problems in Figure 3. Most models converge on their respective training sets; however, we observe non-convergence for the FLOORTILE, ROVERS, and SPANNER domains. This lack of convergence is generally reflected in their test-time performance, with the exception of SPANNER. Although training in this domain is unstable—potentially due to forgetting or overfitting—the final model nevertheless exhibits strong generalization.

We hypothesize that this behavior is specific to the structure of the SPANNER domain. In particular, there exists a simple but suboptimal greedy strategy that involves picking up every spanner encountered. While this strategy is not optimal, it generalizes remarkably well. In contrast, attempting to learn an optimal policy eliminates this greedy behavior, which may hinder generalization. This suggests a broader challenge for domains that admit highly general-

izable greedy strategies but lack an optimal strategy with similar generalization properties. Our training procedure explicitly aims to converge to the optimal general policy, which may explain the observed instability.

A.3. Additional Direct Comparison with Lifted HER

A key baseline we consider is Lifted HER (Ståhlberg & Geffner, 2026), as it employs the same architecture and also targets generalized planning. The main distinction lies in how sparse-reward learning is handled in such domains. Unfortunately, the original work (Ståhlberg & Geffner, 2026) did not evaluate on the learning track of the IPC.

We applied our method to the domains presented in Table 7. In many training runs, the fixed validation set is unable to assess the generalization capabilities of checkpoints accurately, often selecting a sub-par model. Thus, after all fixed validation instances had been evaluated, we extended the checkpoint-selection procedure with additional benchmark test instances to obtain a more stable model selection. These instances were used only for checkpoint selection and never for gradient updates. Overall, the results are comparable to Lifted HER, with a notable advantage in DELIVERY: the original authors reported that Lifted HER struggles due to the low probability of successfully delivering two boxes, a challenge that our method addresses effectively.

A.4. Additional Batch Size Comparisons on Puzzle Domains

The direct comparison of expanded nodes with (Orseau & Lelis, 2021) in Table 3 is not entirely fair, because their search-based rollouts use a batch size of 32. Instead of expanding a single node at a time, their method evaluates, and therefore expands, an entire batch of nodes simultaneously. This design better exploits GPU parallelism, but it also increases the reported expansion counts, since a batch size of 32 imposes a minimum number of expansions per search step. To account for this difference, Table 6 reports results for our models when evaluated with a batch size of 32 at test time. As expected, the number of expanded nodes increases under the larger batch size. At the same time, we observe shorter solution plans on average. Overall, GSP continues to outperform the results reported in (Orseau & Lelis, 2021) while still expanding fewer nodes.

A.5. Fair comparison with Classical Heuristics

LAMA (Richter & Westphal, 2010) is a strong domain-independent classical planner. However, a direct comparison with LAMA is difficult because performance is affected not only by the heuristic itself, but also by implementation and engineering choices, especially under fixed memory and time budgets. To isolate the heuristic contribution, Table 5

compares GSP directly against the classical heuristics h_{ff} and h_{max} within the same execution framework. In all cases, we use WA^* with $w = 2$ and a maximum budget of 10,000 node expansions.

The results show that h_{ff} achieves performance close to LAMA in several domains, whereas h_{max} performs substantially worse. In *miconic*, *rovers*, *satellite*, and *sokoban*, h_{ff} outperforms GSP. These domains appear to benefit from a more exhaustive and consistent symbolic heuristic, especially because they contain many states that are nearly identical at the symbolic level. In such cases, h_{ff} provides more stable heuristic estimates than GSP. Moreover, h_{ff} is often faster: when it fails, it typically reaches the limit of 10,000 expansions, whereas GSP more often fails because of the one-hour timeout.

In the remaining domains, GSP outperforms the classical heuristics. These results suggest that GSP and h_{ff} capture complementary strengths. Combining the learned heuristic with h_{ff} , for example through a multi-queue search strategy similar in spirit to LAMA, is therefore a promising direction for future work.

Algorithm 1 GSP search episode

Require: instance \mathcal{E} , initial state s_0 , transition function \mathcal{T} , heuristic Q_θ , weight w , budget B , dead-end bound R_\perp
Ensure: replay tuples \mathcal{D} of (s, a, R)

- 1: $\mathcal{F} \leftarrow \text{Queue}(\emptyset)$
- 2: $\mathcal{V} \leftarrow \{s_0\}$ *(first-discovery visitation set)*
- 3: $\mathcal{D} \leftarrow \emptyset$
- 4: **for all** $a \in \mathcal{A}(s_0)$ **do**
- 5: $\text{PARENT}(s_0, a) \leftarrow \perp$
- 6: $g(s_0) \leftarrow 0$
- 7: push (s_0, a) into \mathcal{F} with priority $g(s_0) + wQ_\theta(s_0, a)$
- 8: **end for**
- 9: **for** $t = 1$ to B **do**
- 10: **if** $\mathcal{F} = \emptyset$ **then**
- 11: **break**
- 12: **end if**
- 13: pop (s, a) with maximal priority from \mathcal{F}
- 14: $s' \leftarrow \mathcal{T}(s, a)$
- 15: **if** s' is goal **then**
- 16: $R \leftarrow 0$ *(suffix return along goal path)*
- 17: **while** $(s, a) \neq \perp$ **do**
- 18: $R \leftarrow R - 1$
- 19: **if** $(s, a, -\infty) \in \mathcal{D}$ **then**
- 20: remove $(s, a, -\infty)$ from \mathcal{D}
- 21: **end if**
- 22: add (s, a, R) to \mathcal{D}
- 23: $(s, a) \leftarrow \text{PARENT}(s, a)$
- 24: **end while**
- 25: **return** \mathcal{D}
- 26: **end if**
- 27: **if** $\mathcal{A}(s') = \emptyset$ **then**
- 28: add (s, a, R_\perp) to \mathcal{D} ; **continue**
- 29: **end if**
- 30: add $(s, a, -\infty)$ to \mathcal{D} *(unbounded bootstrap sample)*
- 31: **if** $s' \notin \mathcal{V}$ **then**
- 32: $\mathcal{V} \leftarrow \mathcal{V} \cup \{s'\}$;
- 33: **for all** $a' \in \mathcal{A}(s')$ **do**
- 34: $\text{PARENT}(s', a') \leftarrow (s, a)$
- 35: $g(s') \leftarrow g(s) - 1$
- 36: push (s', a') into \mathcal{F} with priority $g(s') + wQ_\theta(s', a')$
- 37: **end for**
- 38: **end if**
- 39: **end for**
- 40: **return** \mathcal{D}

Domain	GSP $_{\pi}$		GSP $_{WA^*}$			WA $^*_{h_{ff}}$			WA $^*_{h_{max}}$		
	Cov.	Steps	Cov.	Exp.	Steps	Cov.	Exp.	Steps	Cov.	Exp.	Steps
blocksworld	100%	444	79%	29	29	12%	2159	34	3%	702	13
childsnaek	41%	31	29%	-	-	0%	-	-	0%	-	-
ferry	87%	422	77%	110	110	67%	480	115	6%	1076	11
floortile	20%	54	28%	42	42	8%	3599	43	0%	-	-
miconic	100%	490	98%	566	268	100%	840	288	20%	1802	12
rovers	24%	380	11%	245	17	31%	82	17	6%	2053	11
satellite	61%	134	33%	234	18	67%	24	18	6%	1248	7
sokoban	14%	18	32%	556	29	34%	194	31	23%	607	18
spanner	100%	216	27%	981	14	33%	64	12	32%	483	12
transport	73%	448	57%	29	28	34%	728	34	7%	1573	8

Table 5. Results on 2023 IPC benchmark. We report coverage (‘Cov.’ fraction of 90 test instances solved) and average plan length (Steps) over solved instances for GSP as a greedy policy (GSP $_{\pi}$) and as a WA * ($w = 2$) heuristic (GSP $_{WA^*}$), alongside h_{ff} and h_{max} . For GSP $_{WA^*}$ and WA $^*_{h_{ff}}$, expanded nodes (Exp.) and plan length (Steps) are reported only on problems solved by both GSP $_{WA^*}$ and WA $^*_{h_{ff}}$. For WA $^*_{h_{max}}$, Exp. and Steps are reported on problems solved by both GSP $_{WA^*}$ and WA $^*_{h_{max}}$. The search budget (also for h_{ff} and h_{max}) for each instance is limited to 10,000 expansions or one hour, whichever occurs first.

Domain \rightarrow	Sokoban / The Witness			
Model	Solved	Length	Expansions	Time (s)
GSP $_{GBFS}$	998/1000	38.5/16.2	564/496	59.7/84.0
GSP $_{WA^*, w=2}$	1000/1000	36.0/16.0	207/548	22.1/94.2
GSP $_{GBFS, b=32}$	1000/1000	32.6/14.7	1028/722	103/72.0
GSP $_{WA^*, w=2, b=32}$	1000/1000	32.5/14.7	972/765	61.1/78.7
GBFS (\dagger)	914/290	37.7/13.3	5040/10128	49.2/44.6
WA $^*, w = 2$ (\dagger)	1000/835	35.6/14.2	3298/14305	22.8/55.5
PHS * (\dagger)	1000/1000	37.6/14.4	1522/191	11.3/1.7
LevinTS (\dagger)	1000/1000	40.1/14.8	2640/220	19.5/1.6
PHS $_h$ (\dagger)	1000/1000	38.9/14.6	1962/222	14.8/1.8

Table 6. Batch-size-adjusted comparison on puzzle domains: Sokoban (10×10 , 4 boxes) / The Witness (5×5). ‘Solved’ is the number of solved instances out of 1000 per domain. Length, Expansions, and Time report averages over the solved instances in each domain. Sokoban models were trained on the same training problems as Orseau & Lelis (2021). All domains are converted to PDDL with relational encoding. The symbol \dagger refers to Orseau & Lelis (2021). The GSP budget for each instance is limited to 100,000 expansions or five hours, whichever occurs first. For GSP $_{b=32}$, we use a batch size of 32 to enable a fairer comparison against Orseau & Lelis (2021), whose results are also reported with a batch size of 32.

Domain	GSP $_{\pi}$		GSP $_{WA^*}$		Lifted HER		Propositional HER		LAMA	
	Cov.	Steps	Cov.	Steps	Cov.	Steps	Cov.	Steps		
blocks	100%	97.9	100%	96.5	100%	96.7	100%	107.3	100%	232.5
childsnaek	79%	89.3	34%	59.4	56%	77.8	100%	92.6	100%	98.4
delivery	93%	293.3	42%	134.7	12%	292.2	11%	167.0	99%	276.1
gripper	100%	238.0	74%	202.6	100%	238.0	100%	239.0	100%	238.0
miconic	100%	158.0	100%	158.0	100%	160.0	100%	158.4	100%	195.6
reward	75%	119.3	99%	94.2	58%	95.9	72%	91.6	99%	121.8
spanner	95%	95.3	0%	0.0	100%	95.5	100%	95.5	0%	0.0
visitall	94%	562.4	41%	331.1	100%	453.3	88%	392.6	100%	530.0

Table 7. Benchmark results on the same data as (Stahlberg et al., 2025). We report coverage (Cov.) and average plan length (Steps) for GSP as a greedy policy (GSP $_{\pi}$) and as a WA * ($w = 2$) heuristic (GSP $_{WA^*}$), compared against LIFTED HER and PROPOSITIONAL HER (Stahlberg et al., 2025) and LAMA.

GSP_{π}	<i>Complete</i>		<i>No dead-end supervision</i>		<i>No solution bounds</i>		<i>No sampling strategy</i>	
Domain	Cov.	Steps	Cov.	Steps	Cov.	Steps	Cov.	Steps
blocksworld	83% \pm 24%	410	89% \pm 16%	368	82% \pm 24%	343	63% \pm 16%	284
childsnap	33% \pm 15%	71	53% \pm 12%	279	44% \pm 10%	38	33% \pm 16%	36
ferry	92% \pm 9%	605	83% \pm 11%	435	72% \pm 17%	328	89% \pm 19%	801
floortile	19% \pm 5%	62	29% \pm 6%	93	19% \pm 8%	66	33% \pm 6%	134
miconic	96% \pm 9%	309	84% \pm 15%	195	74% \pm 25%	193	95% \pm 9%	251
rovers	26% \pm 4%	491	24% \pm 5%	475	31% \pm 4%	716	26% \pm 2%	692
satellite	44% \pm 10%	331	53% \pm 6%	241	47% \pm 9%	308	48% \pm 5%	276
sokoban	16% \pm 3%	19	15% \pm 1%	20	19% \pm 2%	20	17% \pm 2%	23
spanner	97% \pm 4%	190	72% \pm 21%	186	36% \pm 5%	22	55% \pm 29%	99
transport	85% \pm 15%	407	76% \pm 11%	542	73% \pm 10%	184	80% \pm 7%	424
GSP_{WA^*}	<i>Complete</i>		<i>No dead-end supervision</i>		<i>No solution bounds</i>		<i>No sampling strategy</i>	
Domain	Cov.	Steps	Cov.	Steps	Cov.	Steps	Cov.	Steps
blocksworld	72% \pm 4%	196	78% \pm 5%	236	78% \pm 7%	235	71% \pm 5%	188
childsnap	23% \pm 14%	23	27% \pm 15%	24	29% \pm 9%	22	27% \pm 15%	24
ferry	67% \pm 0%	110	67% \pm 0%	110	66% \pm 5%	111	68% \pm 2%	119
floortile	32% \pm 2%	59	34% \pm 2%	66	26% \pm 9%	60	35% \pm 2%	72
miconic	81% \pm 9%	141	84% \pm 11%	167	81% \pm 17%	160	89% \pm 11%	199
rovers	8% \pm 3%	20	12% \pm 4%	19	11% \pm 4%	18	11% \pm 3%	19
satellite	27% \pm 9%	15	33% \pm 0%	18	29% \pm 6%	15	33% \pm 1%	17
sokoban	33% \pm 1%	30	32% \pm 0%	30.0	33% \pm 1%	29	33% \pm 1%	30
spanner	26% \pm 2%	14	30% \pm 4%	14	25% \pm 2%	12	31% \pm 2%	14
transport	56% \pm 6%	51	50% \pm 2%	44	46% \pm 2%	35	50% \pm 3%	41

Table 8. IPC-2023 test results for GSP_{π} and GSP_{WA^*} across training variants. *Cov.* denotes the fraction of the 90 test instances solved, reported as mean \pm standard deviation over independently trained models. *Steps* denotes the average plan length over solved instances, averaged across models. GSP_{WA^*} evaluates the learned model with WA^* search using $w = 2$.

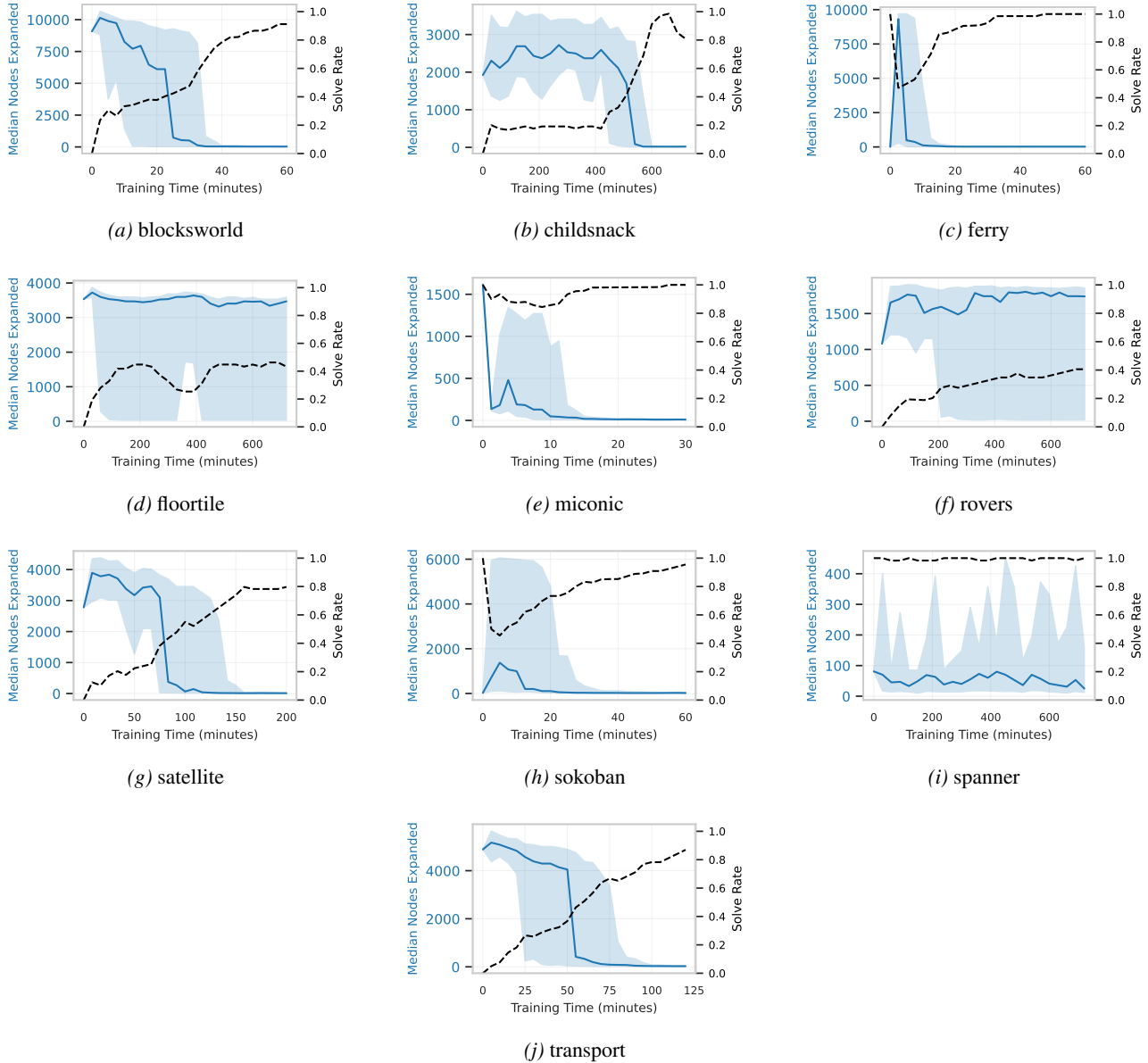


Figure 3. Training progress across all IPC-learning domains. The blue line (left axis) shows the median number of expanded nodes, with shaded regions representing the 25th and 75th percentiles across all instances. The black line (right axis) shows the solve rate, indicating the percentage of problems solved at each point during training. Each training run lasted 12 hours (720 minutes), and we truncated the plots for runs considered converged.